Environmental Pollution 260 (2020) 114011

Contents lists available at ScienceDirect

Environmental Pollution

journal homepage: www.elsevier.com/locate/envpol

Toxicogenomics provides insights to toxicity pathways of neonicotinoids to aquatic insect, *Chironomus dilutus*☆

Fenghua Wei [a, b, c], Dali Wang [b], Huizhen Li [b], Pu Xia [d], Yong Ran [a], Jing You [b, *]

[a] State Key Laboratory of Organic Geochemistry, Guangzhou Institute of Geochemistry, Chinese Academy of Sciences, Guangzhou, 510640, China
[b] Guangdong Key Laboratory of Environmental Pollution and Health, School of Environment, Jinan University, Guangzhou, 511443, China
[c] University of Chinese Academy of Sciences, Beijing, 100049, China
[d] Department of Biology, University of Ottawa, Ontario, K1N 6N5, Canada

ARTICLE INFO

Article history:
Received 9 November 2019
Received in revised form
3 January 2020
Accepted 16 January 2020
Available online 17 January 2020

Keywords:
Mitochondrial dysfunction
Biological potency distribution curve
Sensitive pathway
Oxidative stress
Neonicotinoid insecticides

ABSTRACT

Neonicotinoid insecticides have posed a great threat to non-target organisms, yet the mechanisms underlying their toxicity are not well characterized. Major modes of action (MoAs) of imidacloprid were analyzed in an aquatic insect *Chironomus dilutus*. Lethal and sublethal outcomes were assessed in the midges after 96-h exposure to imidacloprid. Global transcriptomic profiles were determined using *de novo* RNA-sequencing to more holistically identify toxicity pathways. Transcriptional 10% biological potency values derived from ranked KEGG pathways and GO terms were 0.02 (0.01–0.08) (mean (95% confidence interval) and 0.05 (0.04–0.06) μg L^{-1}, respectively, which were more sensitive than those from phenotypic traits (10% lethal concentration: 0.44 (0.23–0.79) μg L^{-1}; 10% burrowing behavior concentration: 0.30 (0.22–0.43) μg L^{-1}). Major MoAs of imidacloprid in aquatic species were identified as follows: the activation of nicotinic acetylcholine receptors (nAChRs) induced by imidacloprid impaired organisms' nerve system through calcium ion homeostasis imbalance and mitochondrial dysfunction, which posed oxidative stress and DNA damage and eventually caused death of organisms. The current investigation highlighted that imidacloprid affected *C. dilutus* at environmentally relevant concentrations, and elucidated toxicity pathways derived from gene alteration to individual outcomes, calling for more attention to toxicity of neonicotinoids to aquatic organisms.

1. Introduction

Neonicotinoid insecticides have been extensively used all over the world and are readily soluble and quite stable in water, thus they are ubiquitous in aquatic environment, posing considerable risks to non-target organisms (Hladik et al., 2018). Neonicotinoids interfere with the central nervous system of insects through activating nicotinic acetylcholine receptors (nAChRs), leading to overstimulation, paralysis, and death (Matsuda et al., 2001). Although the main modes of actions (MoAs) of neonicotinoids to target species have been well characterized, recent findings of unintended effects of neonicotinoids on non-target organisms raised emerging concerns on additional MoAs of these compounds.

As a consequence of detrimental diffuse nervous system, neonicotinoids negatively affect ventilation and locomotion behaviors of *Chironomus riparius* (Azevedo-Pereira et al., 2011). Neonicotinoids also damage learning and memory of honeybee, leading to altered flight and foraging behaviors (Fischer et al., 2014; Girolami et al., 2009). Furthermore, neonicotinoids may induce endocrine disruption (Qi et al., 2013), mitochondrial dysfunction (Nicodemo et al., 2014), oxidative stress (Qi et al., 2018), and immunodeficiency (Brandt et al., 2017) in various invertebrates. As such, for better predicting adverse effects of neonicotinoids to non-target aquatic species, it is imperative to characterize their underlying molecular mechanisms. However, such information is quite fragmentary to date, calling for more integrative understanding of toxicity mechanisms for neonicotinoids to non-target aquatic species.

High-throughput transcriptome sequencing technology (RNA-Seq) has become a powerful tool for investigating molecular effects of chemicals in a holistic manner and it provided an early warning for ecological risk assessments of hazardous substances (Wang et al., 2009). Based on this technique, ecotoxicogenomics has

☆ This paper has been recommended for acceptance by Dr. Sarah Harmon.
* Corresponding author.
E-mail address: youjing@jnu.edu.cn (J. You).

https://doi.org/10.1016/j.envpol.2020.114011
0269-7491/

shown to be effective in identifying biomarkers and elucidating toxic mechanisms of chemicals to ecologically relevant species, such as invertebrates (Iguchi et al., 2005). However, most of omics-based studies were conducted using a narrow concentration range reaching to phenotypically effective concentrations (Thomas et al., 2012). Information on early altered genes and toxicity pathways at environmentally relevant concentrations was lacking. To effectively integrate omics techniques into ecological risk assessment, it is urgently needed to develop repeatable dose-dependent protocols for toxicity testing. Recently, advanced dose-response modeling based on biological potency distribution curve (BDC) for the omics data was proposed by Xia et al. (Xia et al., 2017; Zhang et al., 2018), In BDC, the gene- and pathway-level points of departure ($POD_{gene\ or\ path}$) were proportionally ranked and fitted into a four-parameter concentration-effect curve. The ranked POD_{path} method could help identifying potentially sensitive pathway profiles in organisms induced by xenobiotics and provide a means for quantifying omics data, so that omics data could serve ecological risk assessment. Chironomid larvae which are the dominating invertebrates in freshwater ecosystems and serve as natural baits for a variety of animals, played an important role in ecological functions (Armitage et al., 1995; Taenzler et al., 2007). Furthermore, midges are sensitive to neonicotinoids compared with many aquatic invertebrates (Morrissey et al., 2015; Raby et al., 2018a; Raby et al., 2018b, c), therefore, they could serve as a sensitive model species to assess aquatic risk of these insecticides.

In the present study, we used the midge, *C. dilutus* as a model aquatic species to examine lethal and sublethal toxicities and molecular mechanisms of a widely used neonicotinoid, imidacloprid on aquatic organisms. To achieve this goal, phenotypic (lethal, behavior, and organ), cellular, protein, and genetic effects of imidacloprid on *C. dilutus* by utilizing RNA-Seq technology along with other testing approaches at cellular, organ, and individual levels were evaluated. The known MoA was ascertained and additional toxicity pathways of neonicotinoids to the midges were explored. Finally, aquatic risk of imidacloprid at environmentally relevant concentrations was assessed.

2. Materials and methods

2.1. Toxicity testing

The midges, *C. dilutus* were cultured in Jinan University following the standard protocol proposed by the U.S. Environmental Protection Agency (USEPA) (USEPA, 2000). To facilitate toxicity mechanism exploration for neonicotinoids and daily observation of burrowing behavior, the experiment was conduct in water with 0.5-cm layer of clean sand.

Stock solution of imidacloprid (1 mg/mL) was prepared in dimethyl sulfoxide (DMSO). Test water was freshly prepared at nominal concentrations of 0.001, 0.01, 0.1, 0.4, 1, 2, 8, 40, and 80 μg L^{-1} (IMI_1−IMI_9) by dosing appropriate amount of imidacloprid into reconstituted moderately hard water (USEPA, 2000) (0.1% DMSO, v/v). Negative and solvent controls were tested simultaneously. In each 500-mL beaker, clean sand and 300 mL of testing solution were added. Ten 4th instar larvae of *C. dilutus* were randomly introduced into each beaker to initiate the exposure. The 96-h toxicity tests were conducted in five replicates per treatment or control. The organisms were fed on the second day with 4 mg of grinded fish food (BFB-Made, Zhongshan, China, protein ≥40%, fat ≤ 5%, fiber ≤ 8%, ash ≤ 16%) per beaker. Conductivity, pH, temperature, and dissolved oxygen in test solution were monitored daily and ammonia was measured at the beginning and the end of the tests. Water was sampled at 0 and 96 h in triplicate and analyzed for imidacloprid concentrations using HPLC-MS/MS following a previously developed method (Zhang et al., 2017). Detailed procedures for chemical analysis are provided in the Supporting Information and Table S1.

After 96-h exposure, the midges were assessed for toxicity at different levels, from lethal, behavioral, organ, and cellular responses to gene expressions (Table S2). The midge was considered lethal if it could not conduct an S-shaped movement after 15 s of gentle agitation. Burrowing behavior of the midges was recorded daily. At the termination of the testing, surviving midges were sieved from the sand and counted. Cumulative distance, movement state, and rotation ability were documented by tracing the movements of the midges for 5 min using a DanioVision™ EthoVision XT (Noldus, Netherlands). Histological and ultrastructural defects in the fourth segment of midge abdomen were examined using a light microscope (Nikon Eclipse-Ci, Japan) and transmission electron microscopy (TEM) (Hitachi-HT7700, Japan) according to previous methods (Cao et al., 2016; Zhang et al., 2014). The intracellular Ca^{2+} level was quantified using a Fura-2/AM probe (Beyotime, Haimen, China), and mitochondrial function was evaluated by detecting adenosine triphosphate (ATP) level and the activity of mitochondrial respiratory chain complex V (F_oF_1-ATPase). Meanwhile, oxidative state was assessed by determining the levels of H_2O_2, catalase (CAT), and methane dicarboxylic aldehyde (MDA). Detailed procedures for these measurements are provided in the Supporting Information.

2.2. Western blot analysis

Since there is no published genome for *C. dilutus*, it is difficult to clone and sequence genes. As such, the antibodies of *C. dilutus* are not readily available. Thus, *in vitro* protein analyses with the mammal antibodies were conducted. Human neuroblastoma SH-SY5Y cell lines were purchased from Shanghai Institute of Life Sciences, Chinese Academy of Sciences (Shanghai, China). Antibodies were purchased from ZenBio Company (Chengdu, China), including calcium/calmodulin-dependent protein kinase II (CAMK II), Ca^{2+} transporting ATPase plasma membrane 3 (ATP2B3), mitochondria complex V ATPase 6 (ATP6), cAMP-dependent protein kinase A (PKA), phospho-adenosine 5′-adenosine monophosphate (AMP)-activated protein kinase α (p-AMPKα, Thr172), cAMP response element-binding protein (CREB), RAC serine/threonine-specific protein kinase (AKT), phospho-AKT (p-AKT, Ser473), and growth-arrest and DNA-damage-inducible protein α (GADD45α). A protein sequence alignment was conducted between human and other mosquitoes (*Chironomus tepperi* and *Aedes aegypti*) due to the protein sequence of *Chironomus dilutus* could not been obtained at protein databases. The alignment results showed identities were 32.9%−74.1% between human and mosquito (Table S3). Western blotting analysis was conducted following a previous method (Lin et al., 2015). Detailed descriptions for the *in vitro* assays and western blotting are presented in the Supporting Information.

2.3. RNA sequencing analysis

Surviving midge larvae exposed to imidacloprid at concentrations less than 2 μg L^{-1} were subjected to total RNA extraction in duplicate using a RNeasy Mini Kit (Qiagen, Hilden, Germany) according to the manufacturer's protocols. The RNA sequencing was performed on a BGISEQ-500 sequencing platform (Wuhan, China). As shown in Fig. S1, the Pearson correlation analysis between different replicates showed a high correlation with Pearson values > 0.9 (Benesty et al., 2009). As no reference genome is available for *C. dilutus*, *de novo* transcriptome of *C. dilutus* was

assembled, annotated, and validated.

Gene and function enrichment analyses were conducted using two strategies. First, gene expressions were compared between the control and exposure groups to identify differentially expressed genes (DEGs) according a Poisson distribution method (Wang et al., 2010). Genes with an adjusted-p value < 0.05 by controlling false discovery rate (FDR) (Benjamini and Hochberg, 1995; Storey and Tibshirani, 2003) and an absolute value of log2 fold change > 1 in expression were identified as DEGs. Then, functional annotation analysis was performed for the DEGs of each treatment using Kyoto Encyclopedia of Genes and Genomes (KEGG) and Gene Ontology (GO) databases. Second, log2-fold changes of each gene against measured concentrations of imidacloprid were fitted into various concentration-effect models using drc (Ritz and Streibig, 2005) and DoseFinding (Bornkamp et al., 2010) packages in R (Table S4). Genes with significant curve fitting performance ($p < 0.05$) were defined as the concentration-responsive genes (CRGs), which were used to estimate the gene-level point of departure (POD_{gene}) according to different types of concentration-effect curves (Fig. S2). Then, CRGs were matched to the pathways curated in the KEGG and GO databases to derive pathway-level point of departure (POD_{path}) (Farmahin et al., 2017; Thomas et al., 2007). To achieve this, the geometric mean of POD_{gene} of all CRGs in the pathway was determined as the POD_{path} of the pathway when a pathway was matched by at least three CRGs. The POD_{path} values were proportionally ranked and fitted into a four-parameter concentration-effect curve using GraphPad Prism 5.0 (San Diego, CA, USA), and the curve was defined as BDC (Xia et al., 2017). The ranked POD_{path} method could provide potentially sensitive pathway profiles in organisms disrupted by xenobiotics. Eventually, a transcriptome-based potency was derived as the concentration corresponding to the 10% proportion of BDC ($P_{path,10}$).

Validation of RNA-Seq data was performed using real-time quantitative polymerase chain reaction (RT-qPCR) on 21 genes based on gene expressions of DEGs and ranked CRGs (including 10 CRGs, Table S5). More details on RNA-Seq analysis and validation are provided in the Supporting Information.

2.4. Ecological risk assessment

Potential risk of waterborne imidacloprid to *C. dilutus* was evaluated according to a modified risk quotient (RQ) method using both toxicological- and genomics-based thresholds. The RQ was calculated by dividing the measured environmental concentration (MEC) by the predicted 10% effective concentration (PEC_{10}) (Eq. (1)). The MEC was from previously reported data of imidacloprid concentrations in Guangzhou urban waterways (Xiong et al., 2019) and it was as used as an example for assessing potential risk of imidacloprid to *C. dilutus*. The PEC_{10} of imidacloprid could be either 10% effect concentration (EC_{10}) or transcriptional $P_{path,10}$. With the RQ values from field sampling sites, probabilistic RQ distributions were constructed for ecological risk assessment (Solomon et al., 2000).

$$RQ = \frac{MEC}{PEC_{10}} \quad (1)$$

3. Results

3.1. Phenotypic toxicity

Imidacloprid concentrations in test solutions varied little throughout the exposure periods, thus the average measured concentrations at the beginning and end of the tests were used as dose metrics (Tables S6 and S7). Survival and behavior of the midges were impaired by imidacloprid in a concentration-dependent manner (Fig. 1A,B and S3). The 96-h 10% and median lethal concentrations (LC_{10} and LC_{50}) were 0.44 (0.23–0.79) (mean (95% confidence interval) and 3.56 (2.16–5.87) μg L^{-1}, respectively. The 96-h 10% and median effective concentrations (EC_{10} and EC_{50}) for impaired burrowing behavior were 0.30 (0.22–0.43) and 0.68 (0.58–0.80) μg L^{-1}, respectively. Heat maps of movement showed that the distance and range of movement decreased with increasing imidacloprid concentrations (Fig. S3).

Histological analysis showed that imidacloprid caused damage on the gut epithelia, circular muscle, and paraderm in the midgut region of *C. dilutus* (Fig. S4). Ultrastructural analysis also revealed mitochondrial impairments induced by imidacloprid (Fig. 1C–F). Specifically, mitochondria cristae were widened and the color was darkened by imidacloprid at 0.01 ± 0.00 and 0.31 ± 0.03 μg L^{-1}, respectively (Fig. 1D and E). The morphology of mitochondria was altered, manifesting a longer elliptical shape (Fig. 1E). Swell of mitochondria in the inner chamber was noticed in some cases and the cristae disappeared at high concentration (1.77 ± 0.17 μg L^{-1}, Fig. 1F).

3.2. Mitochondrial and oxidative damage

As shown in Fig. 2A, the intracellular Ca^{2+} level was increased to 128% ± 22%–150% ± 19% compared to the control exposure to imidacloprid at 0.31 ± 0.03–1.77 ± 0.17 μg L^{-1} (IMI_4–IMI_6). The ATP production was reduced in a concentration-dependent manner (Fig. 2B). F_0F_1-ATPase showed a little reduction in the higher concentrations (IMI_5,6: 0.84 ± 0.14–1.77 ± 0.17 μg L^{-1}) (Fig. 2C).

Imidacloprid also produced oxidative stress in *C. dilutus* (Fig. 2D–F). H_2O_2 level was significantly elevated with the increase of concentration (Fig. 2D). Subsequently, enzyme activity of CAT was significantly increased in IMI_5 and IMI_6 groups, but no changes in the low exposure groups (Fig. 2E). Besides, concentration of MDA was also increased with the increase of concentration (Fig. 2F).

3.3. Altered protein expression

As shown in Fig. 2G and H, imidacloprid significantly affected the expression and activation of important proteins in the SH-SY5Y cells. CAMK II and ATP2B3 which were involved in the calcium signal pathway were negatively affected by imidacloprid. Expressions of mitochondrial related proteins, ATP6, PKA, and p-AMPKα were decreased. CREB, a key protein in memory and learning was also down regulated. GADD45α which is related to the repair of DNA damage was increased. In addition, the ratio of p-AKT/AKT, a key oxidative stress index was significantly decreased.

3.4. Induced transcriptomic responses

De novo assembling of RNA-Seq data revealed 36,797 unigenes (size range from 200 to 20,377, average 1168), including 11,655 contigs (size range from 200 to 20,377, average 1794), and 25,142 singletons (size range from 200 to 15,542, average 877). As shown in Fig. S5, homology with conserved genes of other insects and arthropods was over 90%. The genes were annotated by seven functional databases (NR, InterPro, Swissprot, KOG, KEGG, GO, and NT) with annotation rates of 50.5%, 48.0%, 46.5%, 46.3%, 45.0%, 19.4%, and 14.8%, respectively. Species distribution based on the ratios of different species annotation is plotted in Fig. S6. The most abundant BLAST hits (51.4%) matched with mosquitoes which are sister clade of Chironomidae, such as *Aedes aegypti* (14.8%), *Culex quinquefasciatus* (10.0%), and *Aedes albopictus* (9.54%).

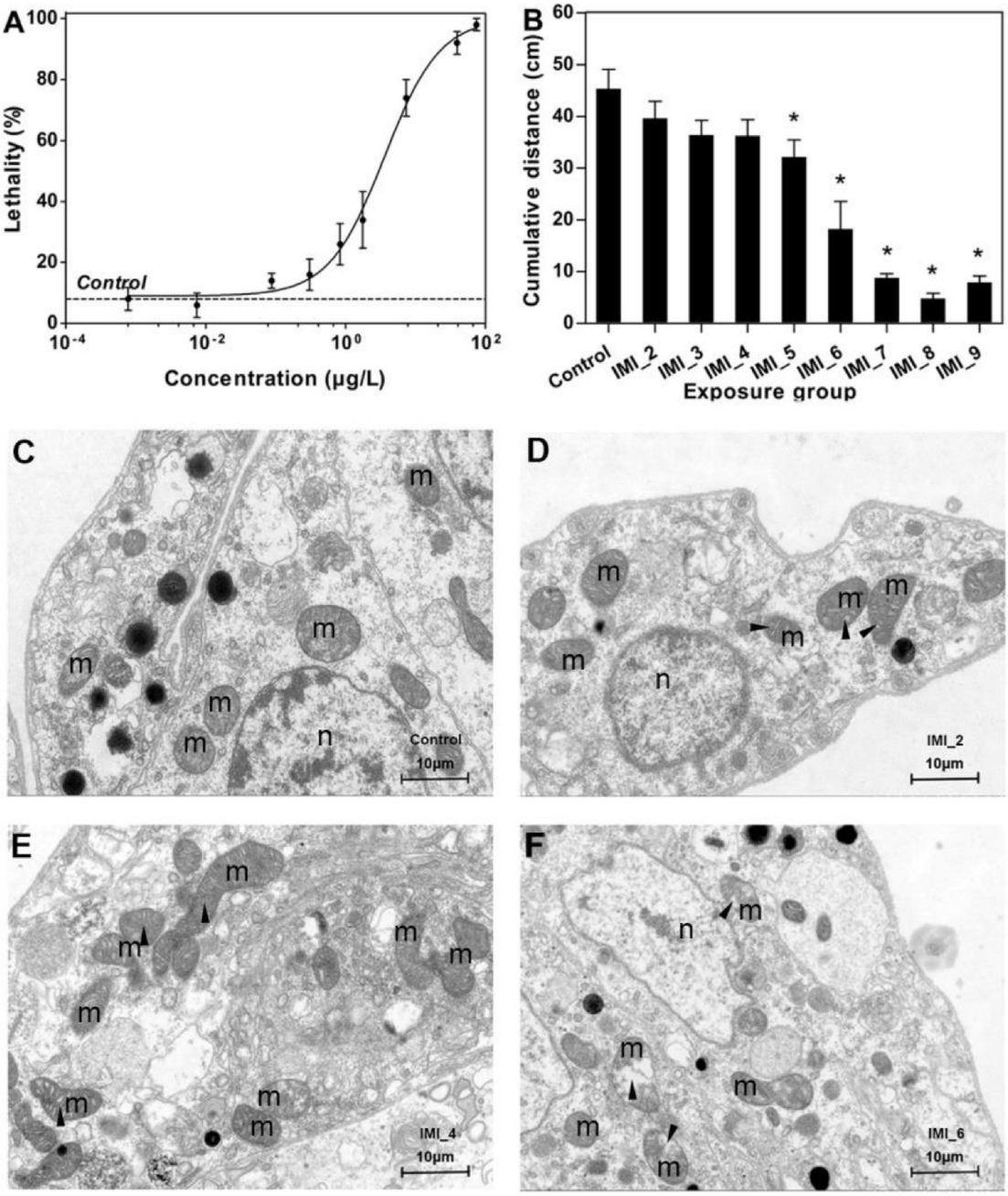

Fig. 1. Lethality, movement, and mitochondrial ultrastructure of *Chironomus dilutus* after 96-h exposure to imidacloprid at different concentrations. (A) Lethality (N = 5); (B) Cumulative distance in 5 min (N = 6). (C–F) Mitochondrial ultrastructure of the fourth segment of the abdomen in the control, IMI_2, IMI_4, and IMI_6, respectively (N = 3). Measured concentrations of IMI_2–IMI_9 were 0.01 ± 0.00, 0.09 ± 0.01, 0.31 ± 0.03, 0.84 ± 0.14, 1.77 ± 0.17, 7.41 ± 0.76, 39.6 ± 2.8, and 74.9 ± 8.5 μg L^{-1}, respectively. The m and n denote mitochondria and nucleus, respectively. Concentration-effect curve was fitted using GraphPad Prism 5.0 software (San Diego, CA, USA). The asterisk denotes significant difference with $p < 0.05$ compared with the control which was assessed with one-way ANOVA using SPSS 17.0 software (Chicago, IL, USA). Data are expressed as mean ± standard error.

Changes of gene expressions in the midges occurred even at the lowest imidacloprid concentration of (7.77 ± 1.40) × 10^{-4} μg L^{-1}. The number of total DEGs in all treatments was 4419 and the number of identified DEGs was 649, 545, 215, 667, 504, and 3352 for the groups IMI_1 to IMI_6 (from (7.77 ± 1.40) × 10^{-4} to 1.77 ± 0.17 μg L^{-1}), respectively (Fig. S6B and Table S8). Imidacloprid at 1.77 ± 0.17 μg L^{-1} (IMI_6) changed the most abundant candidate genes and a total of 80 cytochrome P450 (*cyp*) unigenes were identified in *C. dilutus* with FDR <0.05. As shown in Table S8, 199 CRGs were identified in a significantly dose-dependent manner. The CRGs responsive at low concentrations of imidacloprid were subunit ribosomal proteins (*rps*), cytochrome P450 family 4/6/12 (*cyp 4/6/12*), cathepsin b/l/k (*ctsb/l/k*), NADH-ubiquinone oxidoreductase 2/4 (*nd2/4*), NADP + -dependent farnesol dehydrogenase (*fohsdr*), superoxide dismutase, Cu–Zn family (*sod*), glutathione S-transferase (*gst*), *cat*, and calmodulin (*calm*). In the meantime, RT-qPCR validation of 21 gene responses confirmed high reliability of the transcriptomic data with a good correlation ($R^2 = 0.73$ and $p < 0.0001$) between RNA-Seq and RT-qPCR data (Figs. S7 and S8).

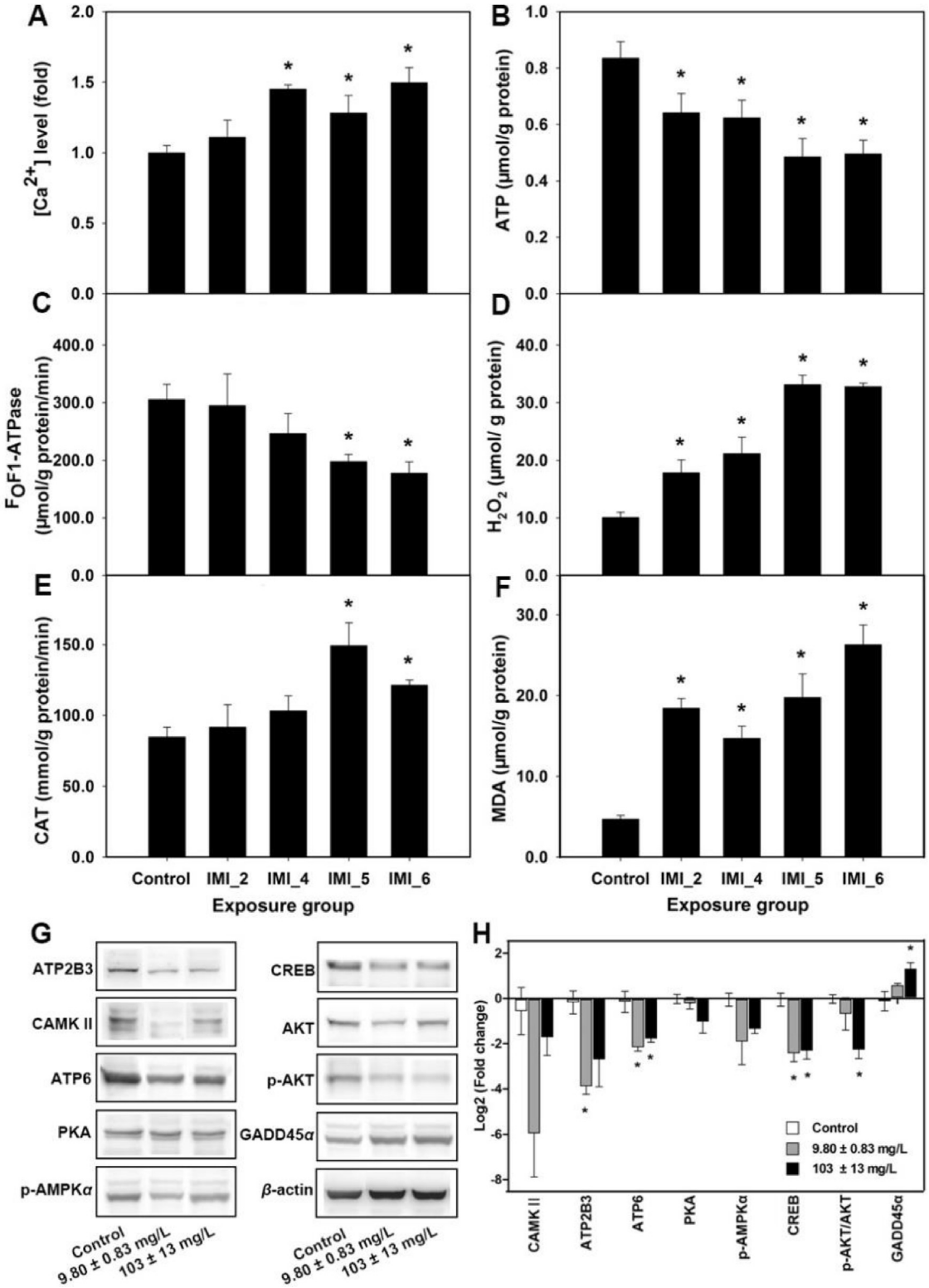

Fig. 2. The calcium ion (Ca^{2+}), mitochondria, and oxidative stress indexes after exposure to imidacloprid. (A–F) Intracellular Ca^{2+} level, adenosine triphosphate (ATP), mitochondrial respiratory chain complex V (F_oF_1-ATPase), H_2O_2, catalase (CAT), and methane dicarboxylic aldehyde (MDA) in *Chironomus dilutus*, respectively. (G) Protein electrophoretograms of the western blotting results in SH-SY5Y cells. (H) Statistical chart of the western blotting results in SH-SY5Y cells. Data are expressed as mean ± standard deviation. The asterisk denotes significant difference with $p < 0.05$ compared with the control which was assessed with one-way ANOVA using SPSS 17.0 software (Chicago, IL, USA). Measured concentrations of IMI_2, 4, 5, 6 were 0.01 ± 0.00, 0.31 ± 0.03, 0.84 ± 0.14, and 1.77 ± 0.17 μg L^{-1}, respectively. CAMK II: Ca^{2+}/calmodulin-dependent protein kinase II; ATP2B3: Ca^{2+} transporting ATPase, plasma membrane 3; ATP6: mitochondria complex V ATPase 6, PKA: cAMP-dependent protein kinase A; p-AMPKα: phospho-adenosine 5′-adenosine monophosphate (AMP)-activated protein kinase (Thr172) α; CREB: cAMP response element-binding protein; AKT: protein kinase B; p-AKT: phospho-AKT (Ser473); GADD45α: growth-arrest and DNA-damage-inducible protein α.

Function annotation of DEGs revealed 36, 36, 34, 36, 45, and 50 top enriched KEGG pathways on neurotoxicity, metabolism and energy homeostasis, and oxidative damage, and 38, 31, 47, 59, 70, and 141 top enriched GO terms in the groups IMI_1 to IMI_6, respectively. Top enriched pathways included calcium signaling, 3′5′-cyclic AMP (cAMP), AMPK, neuroactive ligand-receptor interaction, long-term potentiation (LTP), phosphatidylinositide 3-kinases, phosphatidylinositol-3-kinases/AKT (PI3K/AKT), and p53 pathways (Tables S9–S11 and Fig. 3A). Key DEGs for the enriched KEGG pathways are listed in Table S12. Top enriched GO terms included ribosomal subunit, biosynthetic process, metal ion binding, catalase activity, reactive oxygen species, phosphorylative mechanism, mitochondrial membrane, calcium ion binding, ATP generation from ADP, and oxidation-reduction process (Table S13 and Fig. 3A).

Dose-dependent pathway analysis of CRGs identified 10 KEGG pathways and 20 GO terms (Table S14 and Fig. 3B), which were included in the KEGG pathways and GO terms derived from the DEGs (Fig. S9). According to the BDC curves (Fig. 3B), sensitive pathway profiles were identified. The sensitive pathways included ECM-receptor interaction, mitogen-activated protein kinase (MAPK) signaling pathway, glycerophospholipid metabolism, fatty acid biosynthesis, calcium ion binding, membrane, and ribosome. $P_{path,10}$ values based on KEGG pathway and GO term were derived as 0.02 (0.01–0.08) and 0.05 (0.04–0.06) μg L^{-1}, respectively, which were much lower than midge LC_{10} (0.44 (0.23–0.79) μg L^{-1}) and EC_{10} for inhibited burrowing behavior (0.30 (0.22–0.43) μg L^{-1}), suggesting that $P_{path,10}$ could be used as a more sensitive indicator than the phenotypic indexes.

4. Discussion

Extensive usage of neonicotinoid insecticides has threatened the ecosystem, yet their MoAs have not well characterized so far. In addition, these pieces of information need to be integrated for constructing a toxicity pathways network for more accurately assessing risk of neonicotinoid insecticides. To do so, adverse effects and potential mechanisms of a representative neonicotinoid, imidacloprid, in *C. dilutus* were investigated by RNA-Seq analysis. Besides the known MoA was further confirmed, additional pathways related to mitochondrial dysfunction and oxidative damage were discovered as well. In consistent with previous work (Raby et al., 2018a), the present study demonstrated that 96-h exposure to imidacloprid caused lethal and sublethal effects in *C. dilutus* at environmental concentrations (0.02–3.29 μg L^{-1}) in aquatic environment (Starner and Goh, 2012; Xiong et al., 2019; Zhang et al., 2017).

4.1. Imidacloprid caused behavior disorder by blocking normal neurotransmission

Neonicotinoids act on nAChRs and eventually cause neurotoxicity via damaging the nerve system of organisms (Matsuda et al., 2001). In the present study, intracellular Ca^{2+} levels in *C. dilutus* were significantly elevated after exposure to imidacloprid. In transcriptome analysis, calcium ion binding was likely the early response event as suggested in sensitivity distribution curves derived from the ranked GO terms. The inhibition of the key gene *atp2b* related calcium signaling in transcriptional expression and protein level implied that the accumulated intracellular Ca^{2+} could

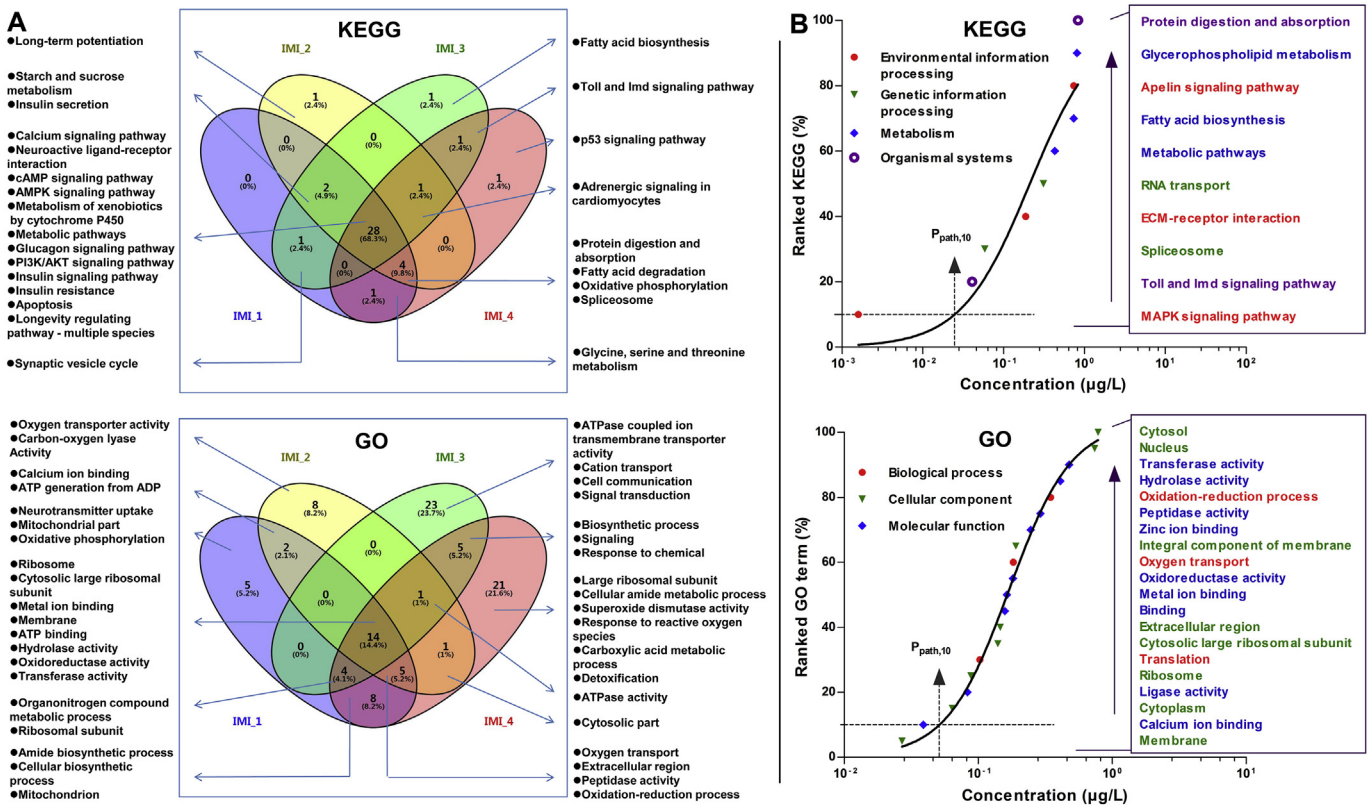

Fig. 3. Venn diagram of top enriched KEGG pathways and ranked GO terms in *Chironomus dilutus* after 96-h exposure to imidacloprid. (A) The enriched KEGG pathways and GO terms in different exposure groups based on differentially expressed genes (DEGs). (B) Biological potency distribution curve (BDC) of the ranked point of departure of KEGG pathways and GO terms (POD_{path}) based on concentration-responsive genes (CRGs). cAMP: 3′,5′-cyclic adenosine monophosphate; AMPK: 5′-AMP-activated protein kinase; PI3K/AKT: phosphatidylinositol- 4,5-bisphosphate 3-kinase/serine/threonine-protein kinase.

not be timely released out of the cells. Wang et al. (2018) reported that Ca^{2+} influx was amplified by imidacloprid as a result of nAChR activation. In another study, Ca^{2+} mobilization in rats was investigated after chronic exposure to imidacloprid, and the intracellular Ca^{2+} level increased from 8.19 in the control to 8.62 mg/dl when body residues of imidacloprid reached 1 mg/kg (Duzguner and Erdogan, 2012). Similarly, intracellular Ca^{2+} influx was significantly evoked by imidacloprid at concentrations greater than 256 μg L^{-1} in the small neurons in rat cerebellar (Kimura-Kuroda et al., 2012). Ca^{2+} signaling responses following activation of nAChRs facilitate the interface with numerous cellular processes (Dajas-Bailador and Wonnacott, 2004), such as signal transduction, cellular proliferation, apoptosis, and production of oxidative stress (Çiğ and Nazıroğlu, 2015). For example, the down-regulation of *camk ii* which showed high identity (69.6%) with *Aedes aegypti*, *calm,* a sensitive CRG, and serine/threonine-protein phosphatase 2B catalytic subunit (*ppp3c*) suggested that the normal Ca^{2+}/calmodulin activated signal transduction might be disrupted in *C. dilutus*. Besides, a previous study has showed that oxidative stress induced by neonicotinoids might be involved in Ca^{2+} homeostasis (Wang et al., 2018).

The disruption of Ca^{2+}/calmodulin activated signal transduction damaged nerve system by blocking normal neurotransmission, impairing behaviors and eventually leading to death of *C. dilutus*. Important neurotoxicity pathways, including neuroactive ligand-receptor interaction and cholinergic synapse were enriched. A previous study has revealed that neonicotinoids inhibited cholinergic neurotransmission in molluscan (*Lymnaea stagnalis*) nervous system (Vehovszky et al., 2015). Hence, neurotoxicity-related muscle paralysis was probably the reason of behavior damage. As discussed above, imidacloprid negatively affected behaviors of many non-target species. For example, ventilation and locomotion of *C. riparius* were damaged by 48-h exposure to imidacloprid at 0.55 and 1.20 μg L^{-1}, respectively (Azevedo-Pereira et al., 2011). Similar effects were also observed for honeybees which lost the capacity of waggling (Eiri and Nieh, 2012) and returning to the feeding sites (Fischer et al., 2014) after exposure to imidacloprid.

4.2. Imidacloprid perturbed metabolism and energy homeostasis

In addition to regular neurotoxicity pathways, metabolism and energy homeostasis in the midges were also perturbed by imidacloprid. Mitochondrial damages were observed in the abdomen cells in midge using ultrastructural analysis. Mitochondrial damages by neonicotinoids have also been previously reported. Thiamethoxam caused reduction of mitochondrial cristae and disorganization of endoplasmic reticulum in *Apis mellifera* (Catae et al., 2014). Similarly, after exposure to thiamethoxam at 0.428 μg $L^{-1}d^{-1}$, morphological and histochemical alterations were observed in honeybees, such as reducing the number of regenerative cells in the epithelium of midgut and cytoplasmic vacuolization (Oliveira et al., 2014). Furthermore, important mitochondrion-related pathways, such as oxidative phosphorylation, ATP binding, and mitochondrion, were enriched by KEGG and GO function analyses. A majority of key genes involved in mitochondrial electron transport chains (ETC) were significantly down-regulated, such as F-type H^+-transporting ATPase subunit a/d (*atpef0a/d*), V-type H^+-transporting ATPase subunit G (*atpev1g*), cytochrome *c* oxidase subunit 2 (*cox2*), *nd2/4*, and succinate dehydrogenase (ubiquinone) flavoprotein subunit (*sdha*). The down-regulation of genes and their corresponding proteins for ETC activity implied potential energy supply deficiency by inhibiting ATP production. Accordingly, imidacloprid significantly reduced F_oF_1-ATPase activity at the concentrations at higher concentrations and inhibited ATP production in *C. dilutus*. This was similar to a study on the toxicity of imidacloprid to honeybees, in which respiratory chain and ATP production in honeybee mitochondria were disrupted (Nicodemo et al., 2014). It has previously reported that imidacloprid impeded mitochondrial function in rats and *Helicoverpa armigera* larvae through inhibiting F_oF_1-ATPase activity (Bizerra et al., 2018; Nareshkumar et al., 2018). Therefore, mitochondrion was an important target site for neonicotinoids and mitochondrial function related genes could be used as key biomarkers for assessing neonicotinoid toxicity.

Mitochondrial dysfunction interfered with Ca^{2+}/calmodulin-dependent cAMP signaling transduction. Two genes, adenylate cyclase 2 (*adcy2*) and guanine nucleotide-binding protein G(s) subunit alpha (*gnas*), were significantly down-regulated, which may interrupt transformation of ATP to cAMP via suppressing adenylate cyclase (AC) activation. Consequently, the activation of PKA might be blocked due to the down-regulation of *pka* gene. As cAMP is the upstream signaling for peroxisome proliferator activated-receptor (PPAR), its disruption might influence PPAR pathway (Chen et al., 2011; Guri et al., 2010), and it is crucial for energy and metabolism balance (Hardie et al., 2012; Kota et al., 2005). Moreover, important genes of PPAR signaling, such as long-chain acyl-CoA synthetase (*acsl*), carnitine O-palmitoyltransferase 1, liver isoform (*cpt1a*), fatty acid-binding protein 3, muscle and heart (*fabp3*), ubiquitin C (*ubc*), and stearoyl-CoA desaturase (Delta-9 desaturase) *(scd*) were also considerably impacted and *ubc* was a CRG, which was further validated by RT-qPCR. In particular, down-regulation of *acsl* indicated decreasing fat acid synthesis, which would lead to a shortage of energy store. Further research on the PPAR disruption by neonicotinoids is needed. In addition, AMPK, another key pathway related to energy and metabolism balance (Hardie et al., 2012; Kota et al., 2005), was also blocked. Especially, mitogen-activated protein kinase kinase 7 (*map3k7*) was significantly down-regulated, which may inhibit AMPK phosphorylation and lead to insufficient energy supply. This was also validated by the decreased expression of p-AMPK in western blotting. Similarly, 0.6 and 6 mg imidacloprid kg^{-1} bw d^{-1} in white adipose tissue of the mice significantly inhibited AMPKα activation due to reducing AMPK phosphorylation (Sun et al., 2017).

Since cAMP/PKA was the upstream event of affecting learning and memory, blocking their activation may damage learning and memory of the organisms (Dajas-Bailador and Wonnacott, 2004). The LTP and dopamine (DA) signaling, which are important pathways associated with learning and memory, were also enriched. The damage of learning and memory was supported by the down-regulation of CREB in both gene and protein levels which may be inhibited by the decreased PKA. This was consistent with previous results that neonicotinoids led to down-regulation of *creb* and *pka* in honey bees (Christen et al., 2016). Besides, *camk ii* gene was heavily implicated in the LTP and DA signaling (Yamauchi, 2005), and its decrease possibly triggered the damage on learning and memory. Previous research revealed that *camk ii* knockdown could affect both early and late phases of olfactory long-term memory in the honeybee (Scholl et al., 2015).

As the metabolism of lipid, carbohydrate, and amino acid was a feedback mechanism for energy deficiency, it could be accelerated in the midges after imidacloprid exposure, which in turn might enhance the detoxification of imidacloprid. As expected, most genes associated with the enriched ribosome and metabolism pathways were significantly up-regulated, revealing that protein synthesis and metabolism increased in the demand for energy supply. Moreover, the affected ribosome was regarded as a sensitive early response by ranked GO analysis. For example, *rp 7/14/15/18// 19/27/30* were found to be sensitive response genes after exposure to imidacloprid at low concentrations. Furthermore, the majority of

cyp*450* genes (such as *cyp2/4/6* genes), which participated in detoxification metabolism of xenobiotics, were significantly altered, especially in the highest exposure group. The *cyp4d1* and *cyp6a2* were also identified as the early response genes by using concentration-response analysis of the genes which were validated by RT-qPCR. The roles of *cyp* genes in detoxification of imidacloprid, such as *cyp6as, cyp9q,* and *cyp6g1*, have been previously reported (De Smet et al., 2017; Derecka et al., 2013; Le Goff et al., 2003). Therefore, *cyp4d1* and *cyp6a2* can also be utilized as the early biomarkers. In addition, *gst* and acylphosphatase (*acyp*), as crucial detoxification genes, were also identified as early responsive to imidacloprid by CRGs analysis with a further validation by RT-qPCR. In summary, transcriptome data revealed possible effects of imidacloprid on ribosome and metabolism related protein synthesis in the midges and this might be one of the toxicity mechanisms of imidacloprid.

4.3. Imidacloprid triggered oxidative damage

One of the consequences of mitochondria dysfunction was overproduction of intracellular reactive oxygen species (ROS), posing oxidative stress on the cells. After the midges being exposed to imidacloprid, two sensitive CRGs, *cat* and *sod* were altered in RNA-Seq and RT-qPCR analyses. In the meantime, elevated H_2O_2 level and CAT enzyme activity were also detected in high concentration groups. Simultaneous detections of these indices confirmed that neonicotinoids induced oxidative stress in *C. dilutus*. These findings were consistent with other investigations. For example, imidacloprid significantly induced CAT enzyme in *D. magna* (Qi et al., 2018). Clothianidin greatly enhanced ROS levels in the earthworm (*Eisenia fetida*) at 0.5 and 1.0 mg kg^{-1}, along with changing SOD and CAT enzyme activities (Liu et al., 2017).

When ROS level was beyond antioxidant defense capacity, it may pose damage on lipid and protein, resulting in lipid peroxidation (Schieber and Chandel, 2014). This was also noted in the midges after imidacloprid exposure, the level of MDA, an indicator for lipid peroxidation in response to oxidative stress, was significantly increased. Chronic exposure to imidacloprid markedly elevated MDA concentrations in liver and plasma of rats (Duzguner and Erdogan, 2012). Subsequently, ROS accumulation would increase mitochondrial permeability, cause functional damage on mitochondria, and finally trigger cell death (Lin and Beal, 2006).

As one of the important response pathways for oxidative stress signaling, disruption of AMPK signaling reduced AKT phosphorylation and altered PI3K/AKT signaling. Gene expressions of *akt* and thrombospondin 2/3/4/5 (*thbs2s*) of PI3K/AKT signaling in the midges were remarkably down-regulated in RNA-Seq and RT-qPCR. The CRG analysis showed *thbs2s* was an early sensitive gene. Meanwhile, the reduction of p-AKT and p-AKT/AKT in protein level validated the inhibition of PI3K/AKT signaling. Similarly, imidacloprid also caused reduction of AKT phosphorylation in mice and human cells (Kim et al., 2013). Therefore, alterations in these pathways indicated that neonicotinoids caused oxidative stress in non-target species, and *akt and thbs2s* genes may serve as potential biomarker genes for imidacloprid.

Accumulation of oxidative stress would trigger pronounced effects on organisms, such as DNA damage, apoptosis, and cell death. As shown in RNA-Seq analysis, p53 signaling, apoptosis, autophagy, and MAPK signaling pathways were disrupted by imidacloprid. On one hand, *gadd45* was significantly up-regulated in gene (RNA-Seq and RT-qPCR) and protein levels. The *gadd45* was an indicator of DNA damage and its induction was linked to repairing DNA damage (Tran et al., 2002). On the other hand, expression of E3 ubiquitin-protein ligase Mdm2 (*mdm2*) was up-regulated and serine/threonine-protein kinase Chk1 (*chk1*) was down-regulated. The alterations of *mdm2* and *chk1* might lead to p53 protein inhibition, and as a result, the repair of DNA damage would fail to be triggered (Haupt et al., 1997). Moreover, poly[ADP-ribose]polymerase (*parp*) was over-expressed in IMI_6 exposure group, suggesting that apoptosis-inducing factor (AIF) in mitochondria was released, which may cause apoptosis and cell death (Yu et al., 2006). It was also found that caspase 7 *(casp 7*) and *ctsb/k/f/d* of apoptosis pathway increased in IMI_6 group. Increasing *casp 7* and *ctsl* (a CRG gene) were validated by RT-qPCR as well. It is noted that these genes were reported to participate in the activation of apoptosis pathway. Similar results have been reported that imidacloprid and clothianidin induced DNA damage and apoptosis through oxidative stress in birds and rats (Bal et al., 2012; Hoshi et al., 2014).

4.4. Putative toxicity pathway development

Based on the key events discussed above, including responses of *C. dilutus* to imidacloprid exposure from phenotypic, biochemical to genetic levels, underlying toxicity pathways of neonicotinoids for aquatic organisms leading to behavior alterations and mortality were proposed (Fig. 4). In these toxicity pathways, imidacloprid blocked neurotransmission and disrupted on energy metabolism, subsequently, induced oxidative damage, even death of organism. First, imidacloprid specifically bound to nAchR and increased intracellular Ca^{2+} level. As a consequence, the neurotransmission that was based on Ca^{2+}/calmodulin mediated signal transduction was blocked, leading to abnormal behaviors of *C. dilutus*. Besides this well-known specific action, additional signaling pathways were also revealed by using the current *de novo* RNA-sequencing approach, which provided a holistic profile of toxicity pathways. Imidacloprid showed potential to interfere with mitochondrial function and thereby the production of ATP via the disruption of Ca^{2+} signaling. As a result, homeostasis of energy metabolism was disturbed, which further blocked the cAMP/PKA signaling transduction and activation of AMPK and LTP and impaired the organisms' ability of learning and memory. At last, the above toxicity effects would induce oxidative stress, which may invoke DNA damage and mortality of individuals. Biochemical responses, although not directly causal to individual toxicity, can help identify chemicals operating via the nAchRs toxicity pathways. Therefore, the toxicity pathways network constructed with imidacloprid as a representative compound is predictive of the toxicity of other neonicotinoids and new substances with similar toxic mechanisms. Multiple toxicants commonly present as mixtures in the environment (e.g., insecticides and fungicides (Raby et al., 2019)) and joint effect among chemicals with similar toxic mechanism is usually regarded as concentration additive. Therefore, the toxicity pathways of imidacloprid could also help assessing mixture toxicity for neonicotinoids. Finally, the putative toxicity pathways network could help interspecies extrapolation of toxic effects which is a challenge of risk assessment.

4.5. Implication for ecological risk assessment

Neonicotinoids have been frequently detected in freshwater ecosystem worldwide (Starner and Goh, 2012; Xiong et al., 2019; Zhang et al., 2017), calling for better understanding of their aquatic risk. Toxicogenomic data provide more sensitive endpoints compared with traditional ecological risk assessment. At the concentrations reported in aquatic environment (0.02–3.29 μg L^{-1}) (Starner and Goh, 2012; Xiong et al., 2019; Zhang et al., 2017), imidacloprid could induce toxicological effects at transcriptomic level and even behavior damage and mortality to *C. dilutus*. Taking Guangzhou, the largest city in South China as an example, potential risk of imidacloprid to *C. dilutus* was assessed with previously

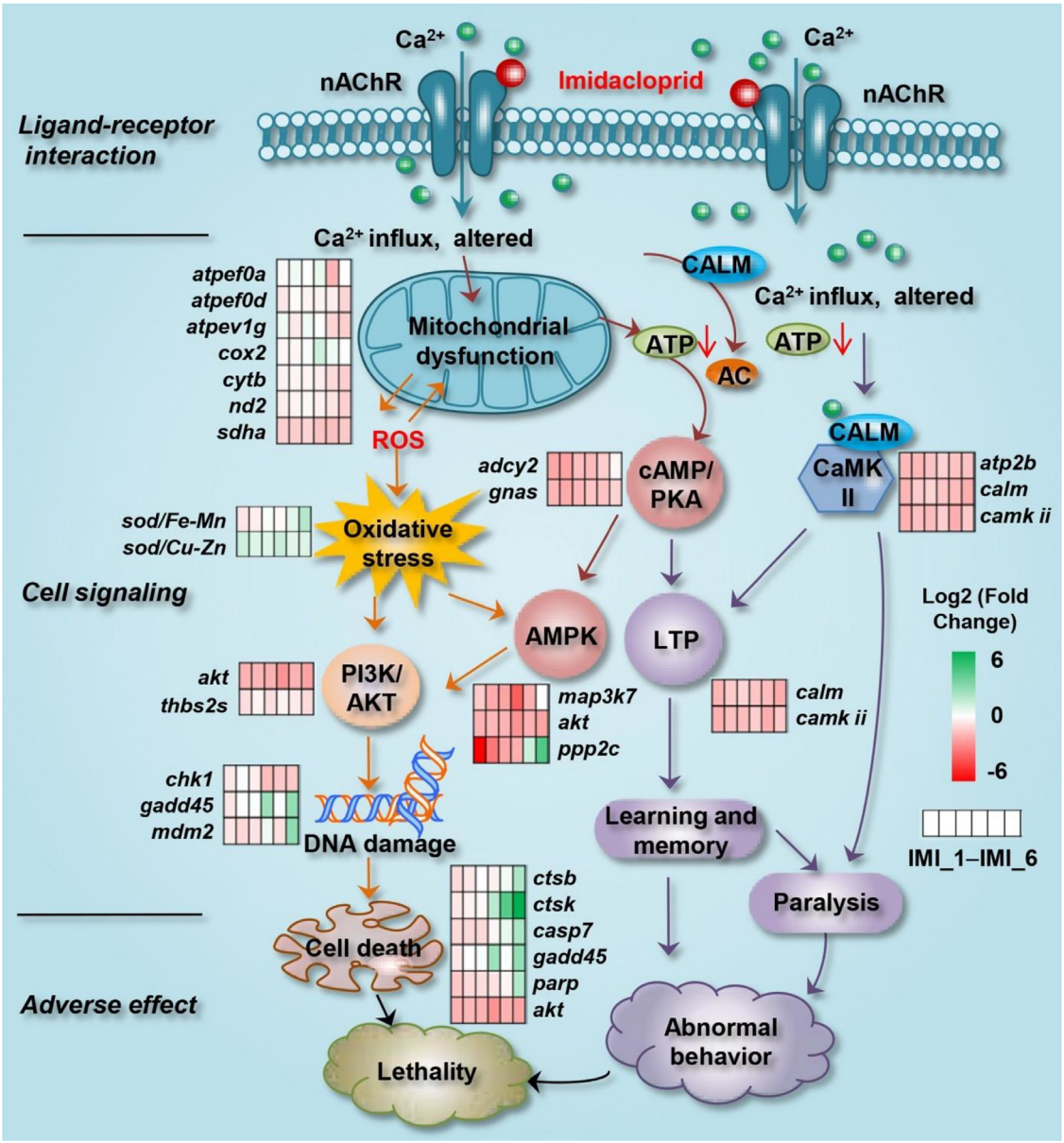

Fig. 4. A putative model illustrating potential toxicity pathways leading to impaired behaviors and lethality in *Chironomus dilutus* after 96-h exposure to imidacloprid. nAChR: nicotinic acetylcholine receptor; TLR: toll-like receptor; CaMK II: calcium/calmodulin-dependent protein kinase II; CALM: calmodulin; AC: adenylate cyclase; cAMP/PKA: 3′5′-cyclic adenosine monophosphate/protein kinase A; LTP: long-term potentiation; ROS: reactive oxygen species; AMPK: 5′ AMP-activated protein kinase; PI3K/AKT: phosphatidylinositol-4,5-bisphosphate 3-kinase/serine/threonine-protein kinase.

reported environmental concentrations of imidacloprid (Xiong et al., 2019). The RQ_{PEC10} based on EC_{10}-lethality, EC_{10}-inhibited burrowing behavior, and $P_{path,10}$ of GO terms in Guangzhou urban waterways were 0.05–0.16, 0.07–0.23, and 0.43–1.32, respectively (Fig. 5). Although acute risk based on conventional endpoints was relatively low, the RQ based on $P_{path,10}$ exceeded 1, indicating possible risk on aquatic invertebrate communities in the study area. This example implied that the $P_{path,10}$ values of toxicogenomic data based on sensitivity distribution curves could be promising early warning thresholds for aquatic risk assessment at the gene expression level. This provided a more sensitive method for ecological risk assessment. Risk assessment using traditional toxicity endpoints (e.g., lethality) may be more operational and realistic for environmental management. In reality, however, many pollutants exist in the environment at extremely low concentrations and would not affect the traditional toxicity endpoints. As a result, risk evaluation based on traditional endpoints might ignore potential risk on the gene-level. So, to include multiple endpoints at different levels would be a direction for future risk assessments.

5. Conclusions

In summary, the RNA-Seq technology was utilized to identify conventional and additional MoAs of imidacloprid to non-target aquatic species, and a putative network of toxicity pathways with newly identified key biomarker genes was constructed. Exposure to imidacloprid led to Ca^{2+} homeostasis imbalance and mitochondria dysfunction through activating the nAChR. Disrupted Ca^{2+} signaling could block cAMP transduction from the ATP, and inhibit

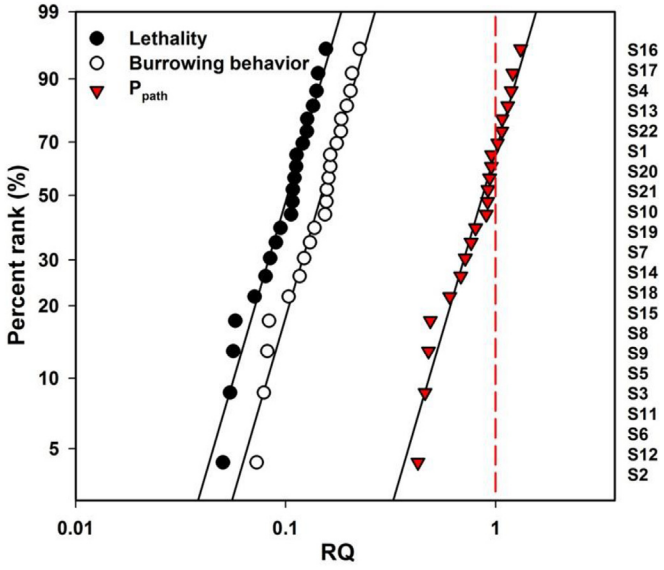

Fig. 5. Risk quotient (RQ) distributions of imidacloprid in water at the sampling sites S1–S22 in Guangzhou urban waterways, China. P_{path}: biological potency based on point of departure of GO terms. The environment concentration in these sampling sites came from previous data (Xiong et al., 2019).

LTP pathway which is related to learning and memory. Furthermore, mitochondria dysfunction could cause oxidative stress and interrupt AMPK signaling. Continuous oxidative stress may induce DNA damage. As an outcome, exposure of *C. dilutus* to imidacloprid could generate apoptosis and cell death, and finally lead to organism death. While more validation studies are necessary to support the results in the current investigation, mitochondrial dysfunction was identified as the potential early warning responses for neonicotinoids, providing an early warning threshold for aquatic risk assessment at the gene expression level.

Declaration of competing interest

The authors declare no conflicts of interest.

CRediT authorship contribution statement

Fenghua Wei: Conceptualization, Methodology, Investigation, Formal analysis, Writing - original draft. **Dali Wang:** Validation, Writing - review & editing. **Huizhen Li:** Investigation, Writing - review & editing. **Pu Xia:** Formal analysis, Writing - review & editing. **Yong Ran:** Writing - review & editing. **Jing You:** Supervision, Conceptualization, Validation, Writing - review & editing, Project administration, Funding acquisition.

Acknowledgements

This work was supported by the National Natural Science Foundation of China (41977343 and 41773101), the Ministry of Science and Technology of China (2017ZX07301005-002), Guangdong Provincial Department of Science and Technology (2017A020216002 and 2015TX01Z168). We appreciate Dr. Jingjing Xiong for help with chemical analysis. This is contribution No. IS-2803 from GIGCAS.

Appendix A. Supplementary data

Supplementary data to this article can be found online at https://doi.org/10.1016/j.envpol.2020.114011.

References

Armitage, P.D., Pinder, L., Cranston, P., 1995. The Chironomidae: Biology and Ecology of Non-biting Midges. Springer Science & Business Media.
Azevedo-Pereira, H., Lemos, M., Soares, A.M., 2011. Effects of imidacloprid exposure on *Chironomus riparius* Meigen larvae: linking acetylcholinesterase activity to behaviour. Ecotoxicol. Environ. Saf. 74, 1210–1215.
Bal, R., Naziroğlu, M., Türk, G., Yilmaz, Ö., Kuloğlu, T., Etem, E., Baydas, G., 2012. Insecticide imidacloprid induces morphological and DNA damage through oxidative toxicity on the reproductive organs of developing male rats. Cell Biochem. Funct. 30, 492–499.
Benesty, J., Chen, J., Huang, Y., Cohen, I., 2009. Pearson Correlation Coefficient, Noise Reduction in Speech Processing. Springer, pp. 1–4.
Benjamini, Y., Hochberg, Y., Controlling the false discovery rate: a practical and powerful approach to multiple testing. J. R. Stat. Soc. Ser. B 57, 289–300.
Bizerra, P.F., Guimarães, A.R., Maioli, M.A., Mingatto, F.E., 2018. Imidacloprid affects rat liver mitochondrial bioenergetics by inhibiting F_oF_1-ATP synthase activity. J. Toxicol. Environ. Health, Part A 81, 229–239.
Bornkamp, B., Pinheiro, J., Bretz, F., 2010. DoseFinding: Planning and Analyzing Dose Finding Experiments. R Project, Vienna, Austria.
Brandt, A., Grikscheit, K., Siede, R., Grosse, R., Meixner, M.D., Büchler, R., 2017. Immunosuppression in honeybee queens by the neonicotinoids thiacloprid and clothianidin. Sci. Rep. 7, 4673.
Cao, F., Zhu, L., Li, H., Yu, S., Wang, C., Qiu, L., 2016. Reproductive toxicity of azoxystrobin to adult zebrafish (*Danio rerio*). Environ. Pollut. 219, 1109–1121.
Catae, A.F., Roat, T.C., De Oliveira, R.A., Ferreira Nocelli, R.C., Malaspina, O., 2014. Cytotoxic effects of thiamethoxam in the midgut and malpighian tubules of *Africanized Apis mellifera* (Hymenoptera: apidae). Microsc. Res. Tech. 77, 274–281.
Chen, Z., Cherng, Yu, B., Chin, Chen, L., Jen, Cheng, K., Chun, Lin, H., Jung, Cheng, J., Tang, 2011. Characterization of the mechanisms of the increase in PPARδ expression induced by digoxin in the heart using the H9c2 cell line. Br. J. Pharmacol. 163, 390–398.
Christen, V., Mittner, F., Fent, K., 2016. Molecular effects of neonicotinoids in honey bees (*Apis mellifera*). Environ. Sci. Technol. 50, 4071–4081.
Çiğ, B., Nazıroğlu, M., 2015. Investigation of the effects of distance from sources on apoptosis, oxidative stress and cytosolic calcium accumulation via TRPV1 channels induced by mobile phones and Wi-Fi in breast cancer cells. Biochim. Biophys. Acta Biomembr. 1848, 2756–2765.
Dajas-Bailador, F., Wonnacott, S., 2004. Nicotinic acetylcholine receptors and the regulation of neuronal signalling. Trends Pharmacol. Sci. 25, 317–324.
De Smet, L., Hatjina, F., Ioannidis, P., Hamamtzoglou, A., Schoonvaere, K., Francis, F., Meeus, I., Smagghe, G., de Graaf, D.C., 2017. Stress indicator gene expression profiles, colony dynamics and tissue development of honey bees exposed to sub-lethal doses of imidacloprid in laboratory and field experiments. PLoS One 12, e0171529.
Derecka, K., Blythe, M.J., Malla, S., Genereux, D.P., Guffanti, A., Pavan, P., Moles, A., Snart, C., Ryder, T., Ortori, C.A., 2013. Transient exposure to low levels of insecticide affects metabolic networks of honeybee larvae. PLoS One 8, e68191.
Duzguner, V., Erdogan, S., 2012. Chronic exposure to imidacloprid induces inflammation and oxidative stress in the liver & central nervous system of rats. Pestic. Biochem. Physiol. 104, 58–64.
Eiri, D.M., Nieh, J.C., 2012. A nicotinic acetylcholine receptor agonist affects honey bee sucrose responsiveness and decreases waggle dancing. J. Exp. Biol. 215, 2022–2029.
Farmahin, R., Williams, A., Kuo, B., Chepelev, N.L., Thomas, R.S., Barton-Maclaren, T.S., Curran, I.H., Nong, A., Wade, M.G., Yauk, C.L., 2017. Recommended approaches in the application of toxicogenomics to derive points of departure for chemical risk assessment. Arch. Toxicol. 91, 2045–2065.
Fischer, J., Mueller, T., Spatz, A.-K., Greggers, U., Gruenewald, B., Menzel, R., 2014. Neonicotinoids interfere with specific components of navigation in honeybees. PLoS One 9, e91364.
Girolami, V., Mazzon, L., Squartini, A., Mori, N., Marzaro, M., Bernardo, A.d., Greatti, M., Giorio, C., Tapparo, A., 2009. Translocation of neonicotinoid insecticides from coated seeds to seedling guttation drops: a novel way of intoxication for bees. J. Econ. Entomol. 102, 1808–1815.
Guri, A.J., Hontecillas, R., Bassaganya-Riera, J., 2010. Abscisic acid synergizes with rosiglitazone to improve glucose tolerance and down-modulate macrophage accumulation in adipose tissue: possible action of the cAMP/PKA/PPAR γ axis. Clin. Nutr. 29, 646–653.
Hardie, D.G., Ross, F.A., Hawley, S.A., 2012. AMPK: a nutrient and energy sensor that maintains energy homeostasis. Nat. Rev. Mol. Cell Biol. 13, 251–262.
Haupt, Y., Maya, R., Kazaz, A., Oren, M., 1997. Mdm2 promotes the rapid degradation of p53. Nature 387, 296.
Hladik, M.L., Main, A.R., Goulson, D., 2018. Environmental risks and challenges associated with neonicotinoid insecticides. Toxicol. Rep. 52, 3329–3335.
Hoshi, N., Hirano, T., Omotehara, T., Tokumoto, J., Umemura, Y., Mantani, Y., Tanida, T., Warita, K., Tabuchi, Y., Yokoyama, T., 2014. Insight into the mechanism of reproductive dysfunction caused by neonicotinoid pesticides. Biol. Pharm. Bull. 37, 1439–1443.
Iguchi, T., Watanabe, H., Katsu, Y., 2005. Application of ecotoxicogenomics for studying endocrine disruption in vertebrates and invertebrates. Environ. Health

Perspect. 114, 101–105.
Kim, J., Park, Y., Yoon, K.S., Clark, J.M., Park, Y., 2013. Imidacloprid, a neonicotinoid insecticide, induces insulin resistance. J. Toxicol. Sci. 38, 655–660.
Kimura-Kuroda, J., Komuta, Y., Kuroda, Y., Hayashi, M., Kawano, H., 2012. Nicotine-like effects of the neonicotinoid insecticides acetamiprid and imidacloprid on cerebellar neurons from neonatal rats. PLoS One 7, e32432.
Kota, B.P., Huang, T.H.-W., Roufogalis, B.D., 2005. An overview on biological mechanisms of PPARs. Pharmacol. Res. 51, 85–94.
Le Goff, G., Boundy, S., Daborn, P., Yen, J., Sofer, L., Lind, R., Sabourault, C., Madi-Ravazzi, L., 2003. Microarray analysis of cytochrome P450 mediated insecticide resistance in *Drosophila*. Insect Biochem. Mol. Biol. 33, 701–708.
Lin, C., Jiang, X., Hu, G., Ko, W.K.W., Wong, A.O.L., 2015. Grass carp prolactin: molecular cloning, tissue expression, intrapituitary autoregulation by prolactin and paracrine regulation by growth hormone and luteinizing hormone. Mol. Cell. Endocrinol. 399, 267–283.
Lin, M.T., Beal, M.F., 2006. Mitochondrial dysfunction and oxidative stress in neurodegenerative diseases. Nature 443, 787–795.
Liu, T., Wang, X., You, X., Chen, D., Li, Y., Wang, F., 2017. Oxidative stress and gene expression of earthworm (*Eisenia fetida*) to clothianidin. Ecotoxicol. Environ. Saf. 142, 489–496.
Matsuda, K., Buckingham, S.D., Kleier, D., Rauh, J.J., Grauso, M., Sattelle, D.B., 2001. Neonicotinoids: insecticides acting on insect nicotinic acetylcholine receptors. Trends Pharmacol. Sci. 22, 573–580.
Morrissey, C.A., Mineau, P., Devries, J.H., Sanchez-Bayo, F., Liess, M., Cavallaro, M.C., Liber, K., 2015. Neonicotinoid contamination of global surface waters and associated risk to aquatic invertebrates: a review. Environ. Int. 74, 291–303.
Nareshkumar, B., Akbar, S.M., Sharma, H.C., Jayalakshmi, S.K., Sreeramulu, K., 2018. Imidacloprid impedes mitochondrial function and induces oxidative stress in cotton bollworm, *Helicoverpa armigera* larvae (Hubner: noctuidae). J. Bioenerg. Biomembr. 50, 21–32.
Nicodemo, D., Maioli, M.A., Medeiros, H.C., Guelfi, M., Balieira, K.V., De Jong, D., Mingatto, F.E., 2014. Fipronil and imidacloprid reduce honeybee mitochondrial activity. Environ. Toxicol. Chem. 33, 2070–2075.
Oliveira, R.A., Roat, T.C., Carvalho, S.M., Malaspina, O., 2014. Side-effects of thiamethoxam on the brain andmidgut of the africanized honeybee *Apis mellifera* (Hymenopptera: apidae). Environ. Toxicol. 29, 1122–1133.
Qi, S., Wang, C., Chen, X., Qin, Z., Li, X., Wang, C., 2013. Toxicity assessments with *Daphnia magna* of guadipyr, a new neonicotinoid insecticide and studies of its effect on acetylcholinesterase (AChE), glutathione S-transferase (GST), catalase (CAT) and chitobiase activities. Ecotoxicol. Environ. Saf. 98, 339–344.
Qi, S., Wang, D., Zhu, L., Teng, M., Wang, C., Xue, X., Wu, L., 2018. Neonicotinoid insecticides imidacloprid, guadipyr, and cycloxaprid induce acute oxidative stress in *Daphnia magna*. Ecotoxicol. Environ. Saf. 148, 352–358.
Raby, M., Maloney, E., Poirier, D.G., Sibley, P.K., 2019. Acute effects of binary mixtures of imidacloprid and tebuconazole on 4 freshwater invertebrates. Environ. Toxicol. Chem. 38, 1093–1103.
Raby, M., Nowierski, M., Perlov, D., Zhao, X., Hao, C., Poirier, D.G., Sibley, P.K., 2018a. Acute toxicity of 6 neonicotinoid insecticides to freshwater invertebrates. Environ. Toxicol. Chem. 37, 1430–1445.
Raby, M., Zhao, X., Hao, C., Poirier, D.G., Sibley, P.K., 2018b. Chronic toxicity of 6 neonicotinoid insecticides to *Chironomus dilutus* and *Neocloeon triangulifer*. Environ. Toxicol. Chem. 37, 2727–2739.
Raby, M., Zhao, X., Hao, C., Poirier, D.G., Sibley, P.K., 2018c. Relative chronic sensitivity of neonicotinoid insecticides to *Ceriodaphnia dubia* and *Daphnia magna*. Ecotoxicol. Environ. Saf. 163, 238–244.
Ritz, C., Streibig, J., 2005. Bioassay analysis using R. J. Stat. Softw. 12, 1–22.
Schieber, M., Chandel, N.S., 2014. ROS function in redox signaling and oxidative stress. Curr. Biol. 24, R453–R462.
Scholl, C., Kübert, N., Muenz, T.S., Rössler, W., 2015. CaMKII knockdown affects both early and late phases of olfactory long-term memory in the honeybee. J. Exp. Biol. 218, 3788–3796.
Solomon, K., Giesy, J., Jones, P., 2000. Probabilistic risk assessment of agrochemicals in the environment. Crop Protect. 19, 649–655.
Starner, K., Goh, K.S., 2012. Detections of the neonicotinoid insecticide imidacloprid in surface waters of three agricultural regions of California, USA, 2010–2011. Bull. Environ. Contam. Toxicol. 88, 316–321.
Storey, J.D., Tibshirani, R., 2003. Statistical significance for genomewide studies. Proc. Natl. Acad. Sci. 100, 9440–9445.
Sun, Q., Qi, W., Xiao, X., Yang, S.-H., Kim, D., Yoon, K.S., Clark, J.M., Park, Y., 2017. Imidacloprid promotes high fat diet-induced adiposity in female C57BL/6J mice and enhances adipogenesis in 3T3-L1 adipocytes via the AMPKα-mediated pathway. J. Agric. Food Chem. 65, 6572–6581.
Taenzler, V., Bruns, E., Dorgerloh, M., Pfeifle, V., Weltje, L., 2007. Chironomids: suitable test organisms for risk assessment investigations on the potential endocrine disrupting properties of pesticides. Ecotoxicology 16, 221–230.
Thomas, R.S., Allen, B.C., Nong, A., Yang, L., Bermudez, E., Clewell III, H.J., Andersen, M.E., 2007. A method to integrate benchmark dose estimates with genomic data to assess the functional effects of chemical exposure. Toxicol. Sci. 98, 240–248.
Thomas, R.S., Himmelstein, M.W., Clewell III, H.J., Yang, Y., Healy, E., Black, M.B., Andersen, M.E., 2012. Cross-species transcriptomic analysis of mouse and rat lung exposed to chloroprene. Toxicol. Sci. 131, 629–640.
Tran, H., Brunet, A., Grenier, J.M., Datta, S.R., Fornace, A.J., DiStefano, P.S., Chiang, L.W., Greenberg, M.E., 2002. DNA repair pathway stimulated by the forkhead transcription factor FOXO3a through the Gadd45 protein. Science 296, 530–534.
USEPA, 2000. Methods for Measuring the Toxicity and Bioaccumulation of Sediment-Associated Contaminants with Freshwater Invertebrates. USEPA.
Vehovszky, Á., Farkas, A., Ács, A., Stoliar, O., Székács, A., Mörtl, M., Győri, J., 2015. Neonicotinoid insecticides inhibit cholinergic neurotransmission in a molluscan (*Lymnaea stagnalis*) nervous system. Aquat. Toxicol. 167, 172–179.
Wang, L., Feng, Z., Wang, X., Wang, X., Zhang, X., 2010. DEGseq: an R package for identifying differentially expressed genes from. RNA-seq data 26, 136–138.
Wang, X., Anadón, A., Wu, Q., Qiao, F., Ares, I., Martínez-Larrañaga, M.-R., Yuan, Z., Martínez, M.-A., 2018. Mechanism of neonicotinoid toxicity: impact on oxidative stress and metabolism. Annu. Rev. Pharmacol. Toxicol. 58, 471–507.
Wang, Z., Gerstein, M., Snyder, M., 2009. RNA-Seq: a revolutionary tool for transcriptomics. Nat. Rev. Genet. 10, 57.
Xia, P., Zhang, X., Zhang, H., Wang, P., Tian, M., Yu, H., 2017. Benchmarking water quality from wastewater to drinking waters using reduced transcriptome of human cells. Environ. Sci. Technol. 51, 9318–9326.
Xiong, J., Wang, Z., Ma, X., Li, H., You, J., 2019. Occurrence and risk of neonicotinoid insecticides in surface water in a rapidly developing region: application of polar organic chemical integrative samplers. Sci. Total Environ. 648, 1305–1312.
Yamauchi, T., 2005. Neuronal Ca^{2+}/calmodulin-dependent protein kinase II—discovery, progress in a quarter of a century, and perspective: implication for learning and memory. Biol. Pharm. Bull. 28, 1342–1354.
Yu, S.-W., Andrabi, S.A., Wang, H., Kim, N.S., Poirier, G.G., Dawson, T.M., Dawson, V.L., 2006. Apoptosis-inducing factor mediates poly (ADP-ribose)(PAR) polymer-induced cell death. Proc. Natl. Acad. Sci. 103, 18314–18319.
Zhang, J., Hu, C.X., Wang, G.H., Li, D.H., Liu, Y.D., 2014. Morphological alterations and acetylcholinesterase and monoamine oxidase inhibition in liver of zebrafish exposed to *Aphanizomenon flos-aquae* DC-1 aphantoxins. Aquat. Toxicol. 157, 215–224.
Zhang, J., Wei, Y., Li, H., Zeng, E.Y., You, J., 2017. Application of Box-Behnken design to optimize multi-sorbent solid phase extraction for trace neonicotinoids in water containing high level of matrix substances. Talanta 170, 392–398.
Zhang, X., Xia, P., Wang, P., Yang, J., Baird, D.J., 2018. Omics Advances in Ecotoxicology, 52. Environ. Sci. Technol., pp. 3842–3851